



## LJMU Research Online

Hamilton, AR, Roberts, M, Hutcheon, GA and Gaskell, EE

**Formulation and antibacterial properties of clay mineral-tetracycline and -doxycycline composites**

<http://researchonline.ljmu.ac.uk/id/eprint/10802/>

### Article

**Citation** (please note it is advisable to refer to the publisher's version if you intend to cite from this work)

**Hamilton, AR, Roberts, M, Hutcheon, GA and Gaskell, EE (2019) Formulation and antibacterial properties of clay mineral-tetracycline and -doxycycline composites. Applied Clay Science, 179. ISSN 0169-1317**

LJMU has developed **LJMU Research Online** for users to access the research output of the University more effectively. Copyright © and Moral Rights for the papers on this site are retained by the individual authors and/or other copyright owners. Users may download and/or print one copy of any article(s) in LJMU Research Online to facilitate their private study or for non-commercial research. You may not engage in further distribution of the material or use it for any profit-making activities or any commercial gain.

The version presented here may differ from the published version or from the version of the record. Please see the repository URL above for details on accessing the published version and note that access may require a subscription.

For more information please contact [researchonline@ljmu.ac.uk](mailto:researchonline@ljmu.ac.uk)

<http://researchonline.ljmu.ac.uk/>

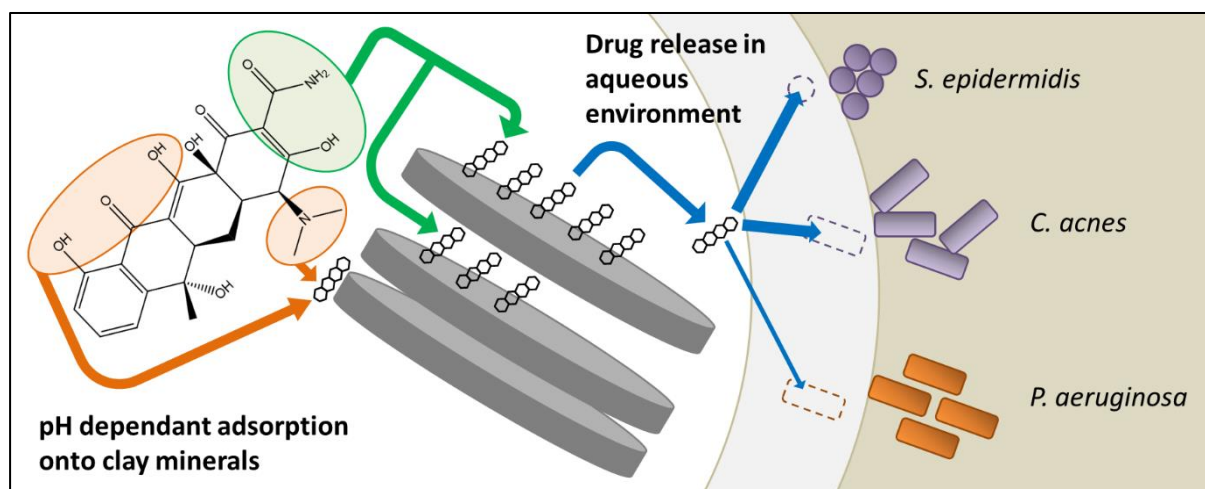
# Formulation and antibacterial properties of clay mineral-tetracycline and -doxycycline composites

Hamilton. A. R., Roberts. M., Hutcheon. G. A., Gaskell. E. E.\*

School of Pharmacy and Biomolecular Sciences, Liverpool John Moores University, Liverpool, UK, L3 3AF

\*Corresponding author. Email address: e.e.gaskell@ljmu.ac.uk

## Graphical Abstract



## Abstract

Clay minerals have been used as adsorbents for decades but research into their use within healthcare as drug-carriers and modified drug release materials is an increasingly common area of interest. In current clinical practice the management of acute bacterial skin and skin-structure infections (ABSSSIs) requires patients to take systemic antibacterial treatment due to a lack of appropriate topical options. In this research tetracycline (TC) and doxycycline (DC) were adsorbed onto a range of clay minerals (kaolinite, montmorillonite, acid-activated montmorillonite, Laponite<sup>®</sup> RD and Laponite<sup>®</sup> XL21) to evaluate their potential as materials for the delivery of these antibiotics to infected wounds. A dispersion pH that favoured the zwitterionic form of the antibiotic molecules was shown to favour adsorption onto the clay minerals. FTIR and pXRD showed that positively charged groups on the antibiotic molecules interacted with the negatively charged clay mineral surface, whilst negatively charged groups on the antibiotic molecules could interact with the positively charged edge-sites of the clay minerals. Swelling clays such as the two Laponites<sup>®</sup> were able to adsorb much more TC and DC due to their structure and chemistry. The clay minerals alone did not have any antibacterial effects against *Staphylococcus epidermidis*, *Cutibacterium acnes*, and

*Pseudomonas aeruginosa*. Antibiotic containing composites successfully released TC and DC, exhibiting activity against the three bacterial strains proportional to the antibiotic-loading on the composites. This research demonstrates the ability of these clay minerals to deliver TC and DC against common skin pathogens and their potential for future development towards clinical applications.

### Highlights

- Adsorption of tetracycline and doxycycline follows pseudo-second order kinetics
- Zwitterionic forms of tetracycline and doxycycline allows maximal adsorption
- Antibiotic molecules adsorbed into the interlayer space of swelling 2:1 clay minerals
- Clay-antibiotic composites were active against *S. epidermidis*, *C. acnes* and *P. aeruginosa*

### Keywords

- Clay Mineral
- Tetracycline
- Doxycycline
- Adsorption
- Antibacterial

### Acknowledgments and Funding

This research forms part of a PhD project and was funded internally through Liverpool John Moores University. Refined montmorillonite, Laponite® RD, and Laponite® XL21 (LapXL21) were donated by BYK Additives Ltd. (Widnes, UK). Doxycycline monohydrate (DC) (>98% by HPLC) was received from Medicis Pharmaceutical (UK). This is accounted for in the methods section of the manuscript.

### Declarations of Interest

The authors have no interests to declare.

## 1. Introduction

Clay minerals are formed of covalently bound sheets of silicon oxide and metal hydroxide in varying proportions. Clay minerals containing an octahedral sheet of metal hydroxide sandwiched between two tetrahedral sheets of silicon oxide, such as montmorillonite and Laponite<sup>®</sup>, are termed 2:1 clay minerals whereas clays with layers formed of one sheet of silicon oxide and a sheet of metal hydroxide are termed 1:1 clay minerals. The 2:1 clay minerals are generally platy in morphology whereas 1:1 clay minerals are either platy, such as kaolinite and dickite, or tubular, such as halloysite (Swartzen-Allen and Matijevic, 1974; Yuan et al., 2015; Zhang et al., 2010).

The structure of 2:1 mineral layers grants them a negative face charge, which is balanced by the presence of exchangeable cations allowing stacks of layers to form into particles. The layers of platy 1:1 clays are bound tightly together through hydrogen bonding to form particles and therefore have a very small interlayer space (Madejova, 2003; Miranda-Trevino and Coles, 2003). This difference in interlayer attraction dictates how the clays behave in aqueous dispersions, with 2:1 clays showing great swelling potential (Swartzen-Allen and Matijevic, 1974; Viseras et al., 2007). The surface charges and exchangeable cations of 2:1 clay minerals allow the adsorption of various cationic species including bacterial cells (Rong et al., 2008; W. Zhao et al., 2012), toxins (Deng et al., 2010), viruses (Lipson and Stotzky, 1983; Schiffenbauer and Stotzky, 1982), and drugs (Viseras et al., 2010). The 1:1 nanotubular clay mineral halloysite has an accessible central lumen that also allows the adsorption of small molecules (Yuan et al., 2015) including drugs (Aguzzi et al., 2013; Ghezzi et al., 2018; Pan et al., 2017; Tan et al., 2014; Wang et al., 2014). The ability of clay minerals to adsorb and desorb a wide range of molecules including water makes them a potentially useful material for the treatment of infected wounds.

Their natural abundance and low toxicity has contributed to their widespread application and has made clay minerals popular materials for drug delivery research. An increasing body of research (Rodrigues et al., 2013; Viseras et al., 2010) is being published on the subject of using clay minerals to deliver a range of antibacterial molecules such as chlorhexidine (Samlíková et al., 2017), ciprofloxacin (Hamilton et al., 2014; Rivera et al., 2016), clindamycin (Porubcan et al., 1978), gentamicin (Rapacz-kmita et al., 2017), vancomycin (Pan et al., 2017), and ofloxacin (Wang et al., 2014), amongst others. The interaction between clay-minerals and drug-molecules is also reported to yield a controlled-release of the adsorbed drug molecules (Park et al., 2008; Rivera et al., 2016), which is attractive for many pharmaceutical applications including patients. However, very little research has looked at utilising phyllosilicate materials as drug-carriers for tetracycline molecules

with the aim of developing novel drug-delivery materials (Chen et al., 2010; Hamilton et al., 2014; Ito et al., 2001).

Tetracyclines inhibit the development, growth and division of bacterial cells through interaction with the 30S subunit of the bacterial ribosome, thus causing inhibition and cessation of protein manufacture (Grassi, 1993; Griffin et al., 2010). Tetracyclines show activity against both Gram-negative and Gram-positive bacteria (Grassi, 1993) but are much more active against Gram-positive bacteria. While used in the treatment of acute bacterial skin and skin structure infections (ABSSSIs) infections (Dawson and Dellavalle, 2013; Sandwell and West Birmingham Hospitals NHS Trust, 2011; The Royal Liverpool and Broadgreen University Hospitals NHS Trust, 2012), more recently, the anti-inflammatory activity of tetracyclines has been investigated for arthritic disease (Greenwald, 2011; Griffin et al., 2010), chronic airway disease (Joks and Durkin, 2011; Raza et al., 2006), and are already used as a steroid-sparing agent in dermatoses (Monk et al., 2011; Tsankov et al., 2003).

However, overprescribing and misuse of tetracyclines – like many other antibiotics – is leading to widespread resistance amongst many common human pathogens (Griffin et al., 2010). The Chief Medical Officer for England (Davies, 2013) and the World Health Organisation (World Health Organization, 2012) have called for new strategies that do not simply revolve around drug discovery but also focus on antimicrobial stewardship and innovating the way we use our current antibacterial arsenal. The development of new, topical, delivery systems for the treatment of wound, skin and skin structure infections could avoid resistance developing within microbiota located in other parts of the body. The development of a topical delivery system for tetracyclines should also reduce the precautions and side effects that need to be considered when prescribing these agents. For example, patients would no longer need to avoid ingesting milk or other polyvalent metallic cation containing products (RPS and BMJ, 2017). It would also be possible to reduce the overall dose required to treat wound, skin and skin structure infections by using topical formulations, and thus systemic absorption would also be reduced. In turn, this will reduce the incidence of general adverse effects such as nausea and vomiting, and more specific adverse effects such as hepatic impairment and antibiotic-associated-diarrhoea from organisms like *Clostridium difficile* (also known as *Clostridioides difficile*) (RPS and BMJ, 2017; Tsankov et al., 2003).

This research investigated and characterised the adsorption of tetracycline and doxycycline onto kaolinite, montmorillonite, montmorillonite K-10, Laponite® RD and Laponite® XL21. Then, appropriate composites were tested against the common ABSSSI pathogens *S. epidermidis*, *C. acnes*,

and *P. aeruginosa* to determine whether these composites could be utilised for healthcare applications.

## 2. Materials and Methods

### 2.1. Materials

Kaolinite (Kaol, cation exchange capacity (CEC) = 3 meq/100 g, specific surface area (SSA) =  $\sim 25$  m<sup>2</sup>/g) washed and sieved, was obtained from Fischer (UK); and acid activated montmorillonite, montmorillonite K-10 (MtK10, CEC = 119 meq/100 g, SSA =  $\sim 250$  m<sup>2</sup>/g) was obtained from Acros (UK). Refined montmorillonite (rMt, CEC = 76 meq/100 g, SSA =  $\sim 600$  m<sup>2</sup>/g) and two synthetic hectorite-like clays, Laponite® RD (LapRD, CEC = 53 meq/100 g, SSA =  $\sim 370$  m<sup>2</sup>/g) and Laponite® XL21 (LapXL21, CEC = 65 meq/100 g, SSA =  $\sim 370$  m<sup>2</sup>/g) were donated by BYK Additives Ltd. (Widnes, UK). Tetracycline hydrochloride (TC) (>98% by HPLC) was obtained from Sigma Aldrich (UK) and doxycycline monohydrate (DC) (>98% by HPLC) was received from Medicis Pharmaceutical (UK).

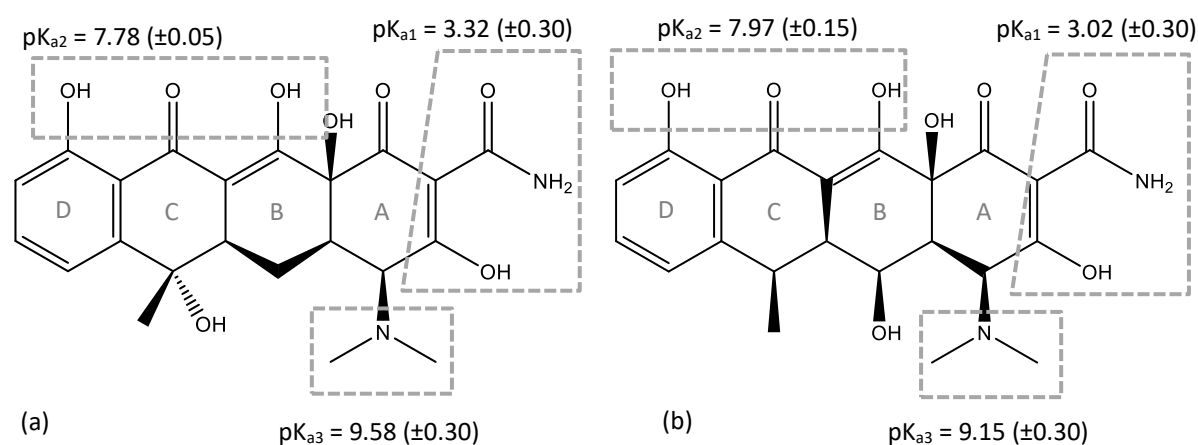


**Figure 1.** Chemical structures and related pK<sub>a</sub> constants for tetracycline (a) and doxycycline (b).

The structures of TC and DC are given in figure 1 along with their three respective pK<sub>a</sub> values. At pH below the pK<sub>a1</sub> the dimethylamino group on the A ring is protonated resulting in a cation (e.g. TCH<sub>3</sub><sup>+</sup> or TC + 0 0). At pH above pK<sub>a1</sub> but below pK<sub>a2</sub> the dimethyl group remains protonated while the hydroxyl group on C3 of the A ring deprotonates to produce a zwitterion (e.g. TCH<sub>2</sub><sup>±</sup>, TC + - 0) that predominates at pH 5.0 for TC and pH 5.5 for DC. The second deprotonation occurs over the ketone system of the B and C rings, as the pH approaches pK<sub>a2</sub> (e.g. TCH<sup>-</sup>, TC + - -). Finally, as the pH increases further (above pK<sub>a3</sub>) the dimethylamino group deprotonates to form a divalent anionic species (e.g. TC<sup>2-</sup>, TC 0 - -) (Chang et al., 2009b; Parolo et al., 2010; Qiang and Adams, 2004).

Bacterial cultures of *S. epidermidis* (NCTC 13360), *C. acnes* (NCTC 737), and *P. aeruginosa* (NCTC 12903) were used to determine antibacterial activity and were obtained from the National Collection of Type Cultures (NCTC; Public Health England, UK). Live cultures of *S. epidermidis* and *P. aeruginosa* were maintained on nutrient agar under aerobic conditions, whereas live cultures of *C. acnes* were maintained on brain-heart infused agar under anaerobic conditions. All bacterial strains were maintained at 37°C.

## 2.2. Adsorption of tetracycline and doxycycline

To determine the effect of dispersion pH, 250 mg of clay mineral was dispersed in 15 mL deionised water for 2 hours at 7000 rpm then 10 mL of a 2.5 mg/mL solution of TC or DC was added and the pH adjusted to between 1 and 12 with dilute HCl and NaOH. After 24 hours mixing, aliquots of the dispersions were centrifuged (EBA20, Hettich Zentrifugen) at 3000 rpm for 10 minutes. Each experiment was undertaken in triplicate. The concentration of antibiotic remaining in supernatant was determined by UV-Visible spectrophotometry (Genesys 10UV, Thermo Scientific) scanning wavelengths between 200 to 400 nm in triplicate.

Adsorption kinetics were determined by dispersing of 500 mg Kaol, 10 mg rMt, 100 mg MtK10, 10 mg LapRD, or 10 mg LapXL21 in 90 mL deionised water. After 2 hours the clay dispersions were adjusted to pH 2.0 and pH 11 for both TC and DC, and pH 5.0 for TC and pH 5.5 for DC. TC and DC were dissolved in deionised water to a concentration of 2 mg in 10 mL and the solutions adjusted to the corresponding pH. The antibiotic solution was added to the clay-mineral dispersion then 1 mL samples were taken at time intervals between 0 and 48 hours. Samples were filtered through 0.2 µm filters (Minisart, UK) and analysed by UV-Vis spectrophotometry to determine the amount of antibiotic remaining in the supernatant. Due to the size of LapRD and LapXL21 particles these samples were flocculated with equal volumes of 10% w/v NaCl solutions immediately before filtration. TC and DC adsorption kinetics were tested against the first, second, pseudo-first, and pseudo-second order models.

Adsorption isotherms were obtained by dispersing 250 mg clay mineral in 15 mL deionised water for 2 hours. Varying concentrations of antibiotic solution was then added to the dispersions to a final volume of 25 mL. Experiments were undertaken in triplicate at pH 2.0 and pH 11.0 for both TC and DC, and at pH 5.0 for TC and pH 5.5 for DC. Adsorption onto Kaol was allowed to take place over a 24

hour period whereas adsorption onto the other clay minerals was over a 4-hour period. Samples were filtered through 0.2  $\mu\text{m}$  filters and analysed as above. The TC and DC adsorption isotherms were applied to the Freundlich, Langmuir, and Temkin isotherm models.

Solid clay-antibiotic composites from the pH-effect and adsorption isotherm experiments were collected by centrifugation and freeze-drying (Heto FD 2.5, at  $-50^{\circ}\text{C}$ ) for further analysis.

### 2.3. Mechanism of TC and DC adsorption

Fourier-Transform Infrared (FT-IR, Perkin Elmer Spectrum BX FT-IR spectrometer with GladiATR attachment) was used to elucidate the interaction between specific TC and DC functional groups and the clay minerals surfaces. Thirty-two scans were run between 4000 to 400  $\text{cm}^{-1}$  with an interval of 1.0  $\text{cm}^{-1}$  and a resolution of 2.0.

Powder X-Ray diffractometry (pXRD) was performed on a Rigaku miniflex (CuK $\alpha$ 1 radiation source,  $\lambda = 0.154 \text{ nm}$ ) was utilised to determine the location of adsorbed TC and DC within the clay mineral structure. Samples were randomly orientated on aluminium discs and scanned five times between 3 and 20 deg  $2\theta$  (0.01 deg/step). The interlayer spacing of each sample was calculated from the  $d_{001}$  value using Rigaku miniflex analysis software.

### 2.4. Antibacterial testing

To standardise the density of bacterial cultures used in these experiments, liquid cultures of the bacteria were grown at  $37^{\circ}\text{C}$  to a turbidity equal to a McFarland 0.5. *S. epidermidis* and *P. aeruginosa* were grown aerobically in nutrient broth and *C. acnes* was grown anaerobically in brain-heart infusion broth. Serial dilutions of the McFarland 0.5 culture were performed and 200  $\mu\text{L}$  of each dilute culture was spread onto pre-poured plates of the appropriate agar (see section 2.1), then grown at  $37^{\circ}\text{C}$  for 24 hours for *S. epidermidis* and *P. aeruginosa*, and 48 hours for *C. acnes*. Individual colonies were counted on plates that did not exhibit confluent growth to determine the approximate colony forming units (CFU, representing active bacteria) per millilitre of the starting McFarland 0.5 culture. The mean cell density in the McFarland 0.5 was found to be  $48.98 \times 10^6$  CFU/mL for *S. epidermidis*,  $70.5 \times 10^7$  CFU/mL for *P. aeruginosa*, and  $74.25 \times 10^6$  CFU/mL for *C. acnes*.

To measure the antimicrobial properties of the composite materials prepared the zone of inhibition testing was chosen. One millilitre of a 1 in 10 dilution of the prepared McFarland 0.5 cultures was added to 19 mL of the appropriate molten agar before being poured into 80 mm petri-dishes and

allowed to completely set. A sterile cork-borer was used to create wells 5 mm in diameter in the set agar.

Fifty microliters of TC and DC solutions at concentrations ranging between 5  $\mu\text{g}/\text{mL}$  and 250  $\mu\text{g}/\text{mL}$  were placed into each well as standards. Unmodified clay mineral 40  $\text{mg}/\text{mL}$  dispersions were investigated as controls in the same way. Clay mineral-TC and -DC composites were chosen depending on their antibiotic-loading to examine the release below, approximate to, and above monolayer coverage (see table 3). The chosen composites were dispersed to a concentration 40  $\text{mg}/\text{mL}$  and 50  $\mu\text{L}$  of these injected into the prepared agar wells. The petri-dishes were incubated under the appropriate conditions and the zones of inhibition measured with digital callipers in five different positions. Each standard, control, and sample was tested in triplicate.

### **3. Results and Discussion**

#### *3.1. Effects of dispersion pH on adsorption*

The pH of the dispersion had marked effects on the adsorption of TC and DC onto the selected clay minerals with the most obvious changes occurring at extremes of pH. The pattern of TC adsorption (data not shown) onto each clay mineral over the pH spectrum were very similar to those observed for DC (figure 2). TC and DC have similar  $\text{pK}_a$  values, and that the charge on these molecules plays an important role on adsorption onto clay minerals.

At pH of 2 or below, TC and DC carry a mono-positive charge which favours adsorption onto the negatively charged clay mineral surface. However, at these pH values a reduction in TC and DC adsorption was observed. Clay minerals are known to degrade in acidic solutions, altering the layer structure and CEC. A small decrease in adsorption onto MtK10 was observed, which may be explained by the increased concentration of protons (present in this clay due to the acid-activation process) in dispersion competing with TC and DC for exchange sites. It is also possible that increased proton concentration reduced antibiotic adsorption by condensation of the Stern layer, followed by flocculation (Segad et al., 2010; Swartzen-Allen and Matijevic, 1974).

When the dispersion pH is between  $\text{pK}_{a2}$  and  $\text{pK}_{a3}$  for TC and DC the dimethyl amino group still retains its positive charge, with the negative charges being located across the A ring and the high density ketone-hydroxyl system on the molecules (Parolo et al., 2010), see figure 1. As the pH of the dispersion is increased above the  $\text{pK}_{a3}$  the dimethyl amino group deprotonates, resulting in a di-negative species with no positive charge (Browne et al., 1980; Chang et al., 2009b). The reduced

adsorption of TC and DC above pH 11 shows that a positive charge is required for significant adsorption to occur onto these clay minerals. It should also be noted that as the pH of the dispersion increases the charge on the edge of the clay mineral layers changes from positive to negative, which would have resulted in further repulsion of negatively charged TC and DC molecules (Lagaly and Ziesmer, 2003; Swartzen-Allen and Matijevic, 1974).

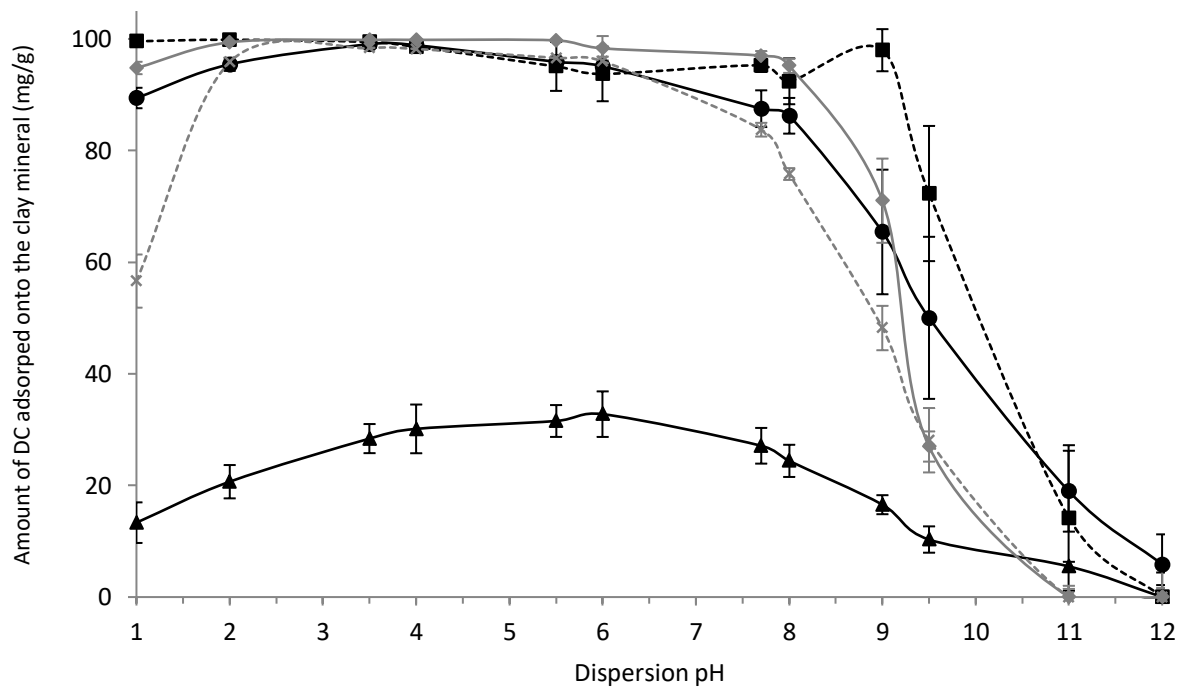


**Figure 2.** Average (mean  $\pm$ SD, n=3) adsorption of DC onto Kaol (triangles), MtK10 (circles), rMt (squares, dashed line), LapRD (diamonds), and LapXL21 (crosses, dashed line) under the influence of dispersion pH.

These data show that a pH between 3.0 and 7.0 is ideal for adsorption of TC and DC onto clay minerals, which was also reported by a number of other research groups (Figuroa et al., 2004; Parolo et al., 2013, 2010). Indeed, when the pH favours increasing proportions of zwitterionic molecules (pH 5.0 for TC and 5.5 for DC) this may promote adsorption onto the clay mineral surface as indicated by the increased adsorption onto Kaol at this pH.

### 3.2. Adsorption kinetics

When experimental data were plotted against the linearised pseudo first and pseudo second order kinetic models the data fitted more closely to the pseudo second order (table 1), which suggests that the adsorption of TC and DC involves two adsorption sites on the clay mineral surface (Kammerer et al., 2011).

The initial rate of adsorption differed greatly depending on the structure of the clay mineral used. The adsorption rate onto MtK10 was one to two orders of magnitude faster than onto Kaol. Clay minerals that were able to swell showed adsorption rates that were a further one to two orders of magnitude faster than MtK10. LapXL21 and LapRD demonstrated an ability to adsorb TC and DC much faster than rMt. In dispersion, LapRD and LapXL21 layers almost completely dissociate at the concentrations used in these studies, resulting in greater available surface areas for interaction with TC and DC (Neumann and Sansom, 1971). It can therefore be assumed that there is less competition for available adsorption sites allowing a much faster initial rate of adsorption.

**Table 1.** Goodness of fit ( $R^2$ ) of selected kinetic orders for the adsorption of TC and DC onto the 5 clay minerals at defined pH, where k is the rate constant.

Clay Mineral	Antibiotic	pH	Pseudo 1 <sup>st</sup> Order	Pseudo 2 <sup>nd</sup> Order		
			( $R^2$ )	( $R^2$ )	Initial rate (mg/g h)	k (g/mg h)
Kaol	TC	2	0.9432	0.9975	110.86	10.56
		5	0.9672	0.9905	40.145	6.25
		11	0.1853	0.9156	62.112	412.87
	DC	2	0.7762	0.9949	65.36	9.43
		5.5	0.6423	0.9957	97.09	7.55
		11	0.9021	0.9672	4.01	27.54
MtK10	TC	2	0.9203	0.9999	3,714	6.52
		5	0.7860	0.9999	3,262	6.33
		11	0.6624	0.9982	228.04	20.50
	DC	2	0.8346	1.0000	14,300	37.39
		5.5	0.6946	0.9999	25,000	62.93
		11	0.9724	0.9998	3,333	14.90
rMt	TC	2	0.9393	0.9999	37,593	1.51
		5	0.7263	0.9999	45,871	2.97
		11	0.0344	0.9987	12,150	16.10
	DC	2	0.7898	0.9997	20,000	1.07
		5.5	0.6548	0.9996	14,285	0.70
		11	0.9495	0.9996	5,000	2.21
LapRD	TC	2	0.5097	0.9999	105,263	3.99
		5	0.1938	0.9999	62,893	3.95
		11	0.0715	0.9999	208,333	12.08
	DC	2	0.7394	0.9999	100,000	4.87
		5.5	0.7791	0.9998	20,000	0.93
		11	0.3898	0.9998	29,000	1.54
LapXL21	TC	2	0.2121	0.9998	78,125	6.05
		5	0.5563	0.9999	69,444	6.03
		11	0.0915	0.9998	90,909	5.97
	DC	2	0.4827	0.9997	25,000	1.42
		5.5	0.1466	0.9999	100,000	7.08
		11	0.1589	0.9997	44,200	39.29

These results confirmed that an acidic environment is more favourable for the adsorption of these two antibiotics, which is also corroborated by the reports from a number of other teams (Chang et al., 2009a; Parolo et al., 2013, 2010). Parolo et al. (2013 and 2010) suggested that the presence of positive charges on TC and DC molecules allows interaction with the negatively charged clay mineral surface. As the pH increases the TC and DC molecules become increasingly negatively charged which can lead to repulsion from the clay mineral surface. At pH 11 the TC and DC molecules are predominantly negatively charged and the edge charges on the clay mineral particles will have transitioned from positive to negative. This results in a system wherein the individual components repel each other, which explains the drop in rate of adsorption observed at this pH (Parolo et al., 2008).

This trend did not however translate to LapRD as it is formulated to buffer at around pH 9, whereas LapXL21 buffers to a more neutral pH. This may result in a positive charge remaining at edge sites of LapRD at higher pH, allowing TC and DC to adsorb onto its edges. The aspect ratio of Laponite® layers is around 1:20 (20 nm diameter, 1 nm thick) so a significant proportion of LapRD surface area is composed of edge sites.

### 3.3. Adsorption isotherms

Adsorption isotherms for TC onto Kaol, MtK10, rMt, and LapXL21 are given in figure 3 and demonstrate the observed effects of pH on absorbance. The Langmuir, Freundlich, and Temkin adsorption models were applied to the isotherm data for both TC and DC onto each of the clay minerals at differing pH (table 2).

The adsorption of TC and DC onto Kaol was shown to fit the Langmuir model more closely, indicating it was a saturable process and a monolayer was formed (Kammerer et al., 2011). The adsorption of TC and DC was greater when the dispersion pH favoured zwitterionic molecules and this was reflected in the monolayer saturation ( $S_m$ , mg/g) values (table 2). The estimated intensity of adsorption ( $b_F$ ) was found to be far greater at pH 11 compared to the lower pH tested indicating the negatively charged TC and DC molecules interact with the edges of Kaol particles more intensely than the faces of the layers.

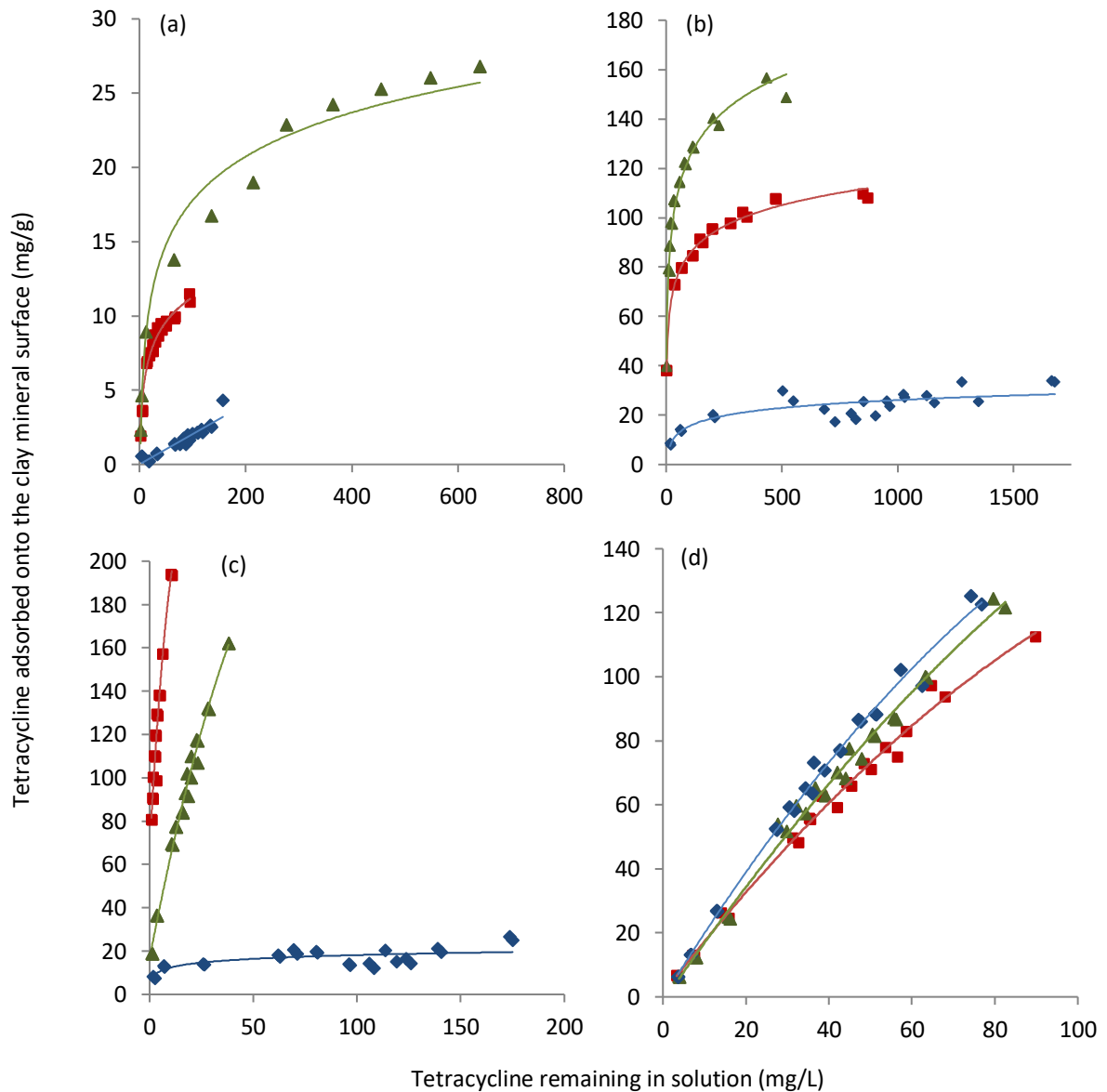


**Figure 3.** Adsorption isotherms (n=3) for the adsorption of TC onto Kaol (a), MtK10 (b), rMt (c), and LapXL21 (d) at pH 2 (squares), pH 5.0 (triangles), and pH 11 (diamonds).

More antibiotic was adsorbed onto MtK10 at a pH that favoured the zwitterionic form of the molecules and resulted in a more concentrated monolayer being formed at the clay mineral surface (Figuroa et al., 2004; Porubcan et al., 1978). The adsorption of TC and DC at pH 2 allowed for good adsorption and a concentrated monolayer but the interaction was less intense than at pH 5 or 5.5. The interaction between the antibiotics and MtK10 was found to be least intense at pH 11, which is reflected in the small amounts of antibiotic adsorbed and the sparsely saturated monolayer estimated through the Langmuir model.

**Table 2.** Correlation of fit between experimental adsorption data to the Langmuir, Freundlich, and Temkin adsorption isotherm models. Where  $S_m$  is the monolayer coverage,  $b_F$  is a dimensionless value for adsorbance intensity, and  $B$  is the heat of adsorption.

Clay Mineral	Antibiotic	pH	Langmuir (R <sup>2</sup> )	Freundlich (R <sup>2</sup> )	Temkin (R <sup>2</sup> )	S <sub>m</sub> (mg/g)	b <sub>F</sub>	B (J/mol)
Kaol	TC	2	0.9811	0.9272	0.8472	10.82	1.93	2.27
		5	0.9719	0.9328	0.9283	25.80	3.10	4.50
		11	0.9811	0.9529	0.9158	3.84	150.45	1.13
	DC	2	0.9128	0.9129	0.9181	7.18	1.80	1.95
		5.5	0.9690	0.8424	0.8246	23.51	1.86	2.87
		11	0.9514	0.7422	0.6403	2.73	187.71	1.22
MtK10	TC	2	0.9443	0.9712	0.9915	94.15	35.62	12.34
		5	0.9587	0.9119	0.9811	123.72	42.01	20.57
		11	0.8839	0.8251	0.7228	25.18	4.21	4.59
	DC	2	0.9557	0.9065	0.9528	94.94	39.69	12.42
		5.5	0.9958	0.9472	0.9523	106.36	19.93	18.36
		11	0.9093	0.9678	0.9715	13.03	7.14	11.51
rMt	TC	2	0.8170	0.9288	0.9016	171.51	79.20	45.84
		5	0.9648	0.9931	0.8623	130.22	16.96	37.41
		11	0.6642	0.6015	0.5011	17.31	7.81	2.51
	DC	2	0.9856	0.9626	0.9918	266.82	59.99	61.06
		5.5	0.9768	0.9214	0.8308	158.65	12.65	33.95
		11	0.9516	0.8516	0.6518	31.46	1.63	6.55
LapRD	TC	2	0.9899	0.9890	0.9057	266.04	6.79	39.10
		5	0.6374	0.7138	0.5370	74.33	1.49	84.87
		11	0.9883	0.9894	0.8939	158.19	7.45	30.43
	DC	2	0.9816	0.9751	0.9205	189.27	11.27	39.51
		5.5	0.9897	0.9859	0.9079	308.45	1.60	72.08
		11	0.9338	0.9190	0.7445	109.04	1.50	25.97
LapXL21	TC	2	0.9947	0.9960	0.8947	227.35	2.27	30.22
		5	0.9977	0.9940	0.8893	238.12	1.60	36.83
		11	0.9951	0.9941	0.9048	78.55	2.00	56.93
	DC	2	0.9784	0.9706	0.8037	215.84	2.79	31.90
		5.5	0.9943	0.9947	0.8457	290.46	1.40	39.26
		11	0.9540	0.9747	0.8513	110.34	1.01	36.72

Adsorption of TC and DC onto rMt showed a number of differences compared to MtK10. The values derived indicate that the adsorption of DC and TC onto rMt is more intense at pH 2, which resulted in a large adsorption of antibiotic and a more saturated monolayer. The structure and chemistry of rMt gives it a high surface charge and a large CEC that can interact more readily with positively charged molecules. These data also suggest the adsorption of TC and DC onto rMt is predominantly via cation exchange as the positively charged molecules will displace the interlayer cations (Chang et al., 2009c).

When the adsorption process was undertaken on LapRD and LapXL21 more antibiotic was adsorbed onto the clay mineral surface and a higher concentration was present within the monolayer at pH

5.0 for TC and pH 5.5 for DC compared to either pH 2 or 11. Layers of LapXL21 and LapRD are more acid-labile than rMt layers (Thompson and Butterworth, 1992), and the resultant decrease specific surface area would have reduced the adsorption capacity of this clay mineral. However, at pH 2 the intensity of interaction was determined to be greater than at pH 5.0 or pH 5.5. Acid dissolution of clay mineral layer structure can also intensify the acid sites present and it may be possible that these sites interact more strongly with the antibiotic molecules. This suggests that cation exchange is not the only process by which TC and DC interact with LapRD and LapXL21 and secondary interactions such as hydrogen-bonding and Van der Waals forces may also be involved (Aguzzi et al., 2005; Parolo et al., 2008).

The heat of adsorption ( $B$ , J/mol) was extremely low in all of these experiments, strengthening the conclusion that the interaction between DC and TC and the clay minerals was by physisorption rather than chemisorption (Itodo and Itodo, 2010; Puttamat and Pavarajarn, 2016). These weak interactions are necessary, however, to allow the antibiotics to desorb from the clay mineral surfaces and impose their effects on bacterial cells.

### 3.4. FTIR analyses

FTIR is a useful technique for identifying functional groups within a compound or mixture and is often used to support the elucidation of drug molecule structures. Molecules, such as TC and DC have individual and characteristic spectra with the majority of absorbance modes being present within the fingerprint region ( $1500$  to  $500$   $\text{cm}^{-1}$ ). Clay minerals also have a number of characteristic modes within this region. The most prominent absorbance around  $1000$   $\text{cm}^{-1}$  is from the Si-O stretch within the tetrahedral sheets. Absorbances lower down the spectra result from M-OH bonds within the octahedral sheets; notably Al-OH at  $912$   $\text{cm}^{-1}$  in KN,  $924$   $\text{cm}^{-1}$  in rMMT, and  $897$   $\text{cm}^{-1}$  in LapXL21 (as a shoulder on the Si-O adsorption); Fe-OH at  $802$   $\text{cm}^{-1}$  and  $685$   $\text{cm}^{-1}$  in rMMT; and Mg-OH at  $607$   $\text{cm}^{-1}$  in KN,  $603$   $\text{cm}^{-1}$  in rMMT, and  $653$   $\text{cm}^{-1}$  in LapXL21 (Madejova, 2003; Tyagi et al., 2006).

As the amount of antibiotic adsorbed increased the amplitude of the absorbances in the TC and DC fingerprint region also increased (figure 4). The characteristic clay mineral Si-O band reduced in intensity but this is unlikely to be due to a change in clay mineral structure as no deformations were observed and is simply a result of the changing antibiotic:clay mineral ratio. The TC and DC O-H/N-H stretching band, which generally appears around  $3350$   $\text{cm}^{-1}$  is masked by the broad O-H band of water at  $3500$   $\text{cm}^{-1}$  (Chang et al., 2009c). This OH band decreased in amplitude as the amount of

antibiotic present within the composites increased, suggesting a loss of hydratable counterbalancing cations as a result of DC and TC adsorption (Madejova, 2003).

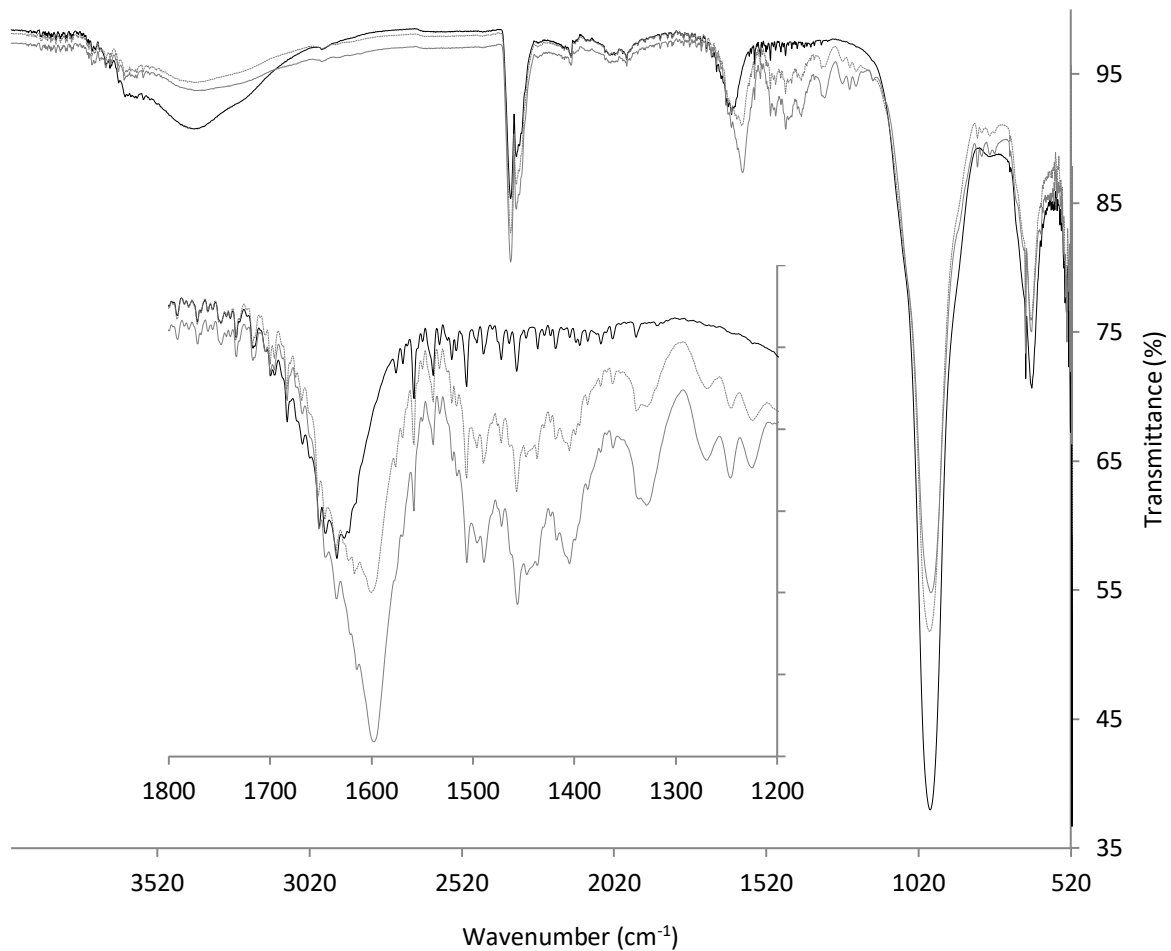


**Figure 4.** FTIR spectra of increasing amounts of DC adsorbed onto LapRD. The lowest DC adsorption (solid black line) and highest adsorption (solid grey line) are presented alongside a DC-LapRD composite whose DC loading is around the monolayer formation point (dashed grey line).

The interaction between DC and TC and the clay mineral surfaces was also confirmed via observed shifts of key absorbances on the FTIR spectra. The absorbance at 1255 cm<sup>-1</sup> is a characteristic C-N stretching vibration, the position of which is known to shift as the pH favours differing charges on the tertiary amine group (de Sousa et al., 2008; Parolo et al., 2010; Y. Zhao et al., 2012). This absorbance shifted from 1255 cm<sup>-1</sup> to 1245 cm<sup>-1</sup> when TC was absorbed onto rMt (figure 5), indicating an interaction between this positively charged group and negatively charged clay mineral faces. Similar shifts were seen for TC and DC onto all the clay minerals tested (data not shown) except at pH 11, where so little antibiotic was adsorbed it was impossible to accurately interpret the

spectra. It is expected that the tertiary amine group on TC deprotonates above pH 9.6 ( $pK_{a3}$ ; pH 9.1 for DC) so this shift in absorbance would be less easily observed.

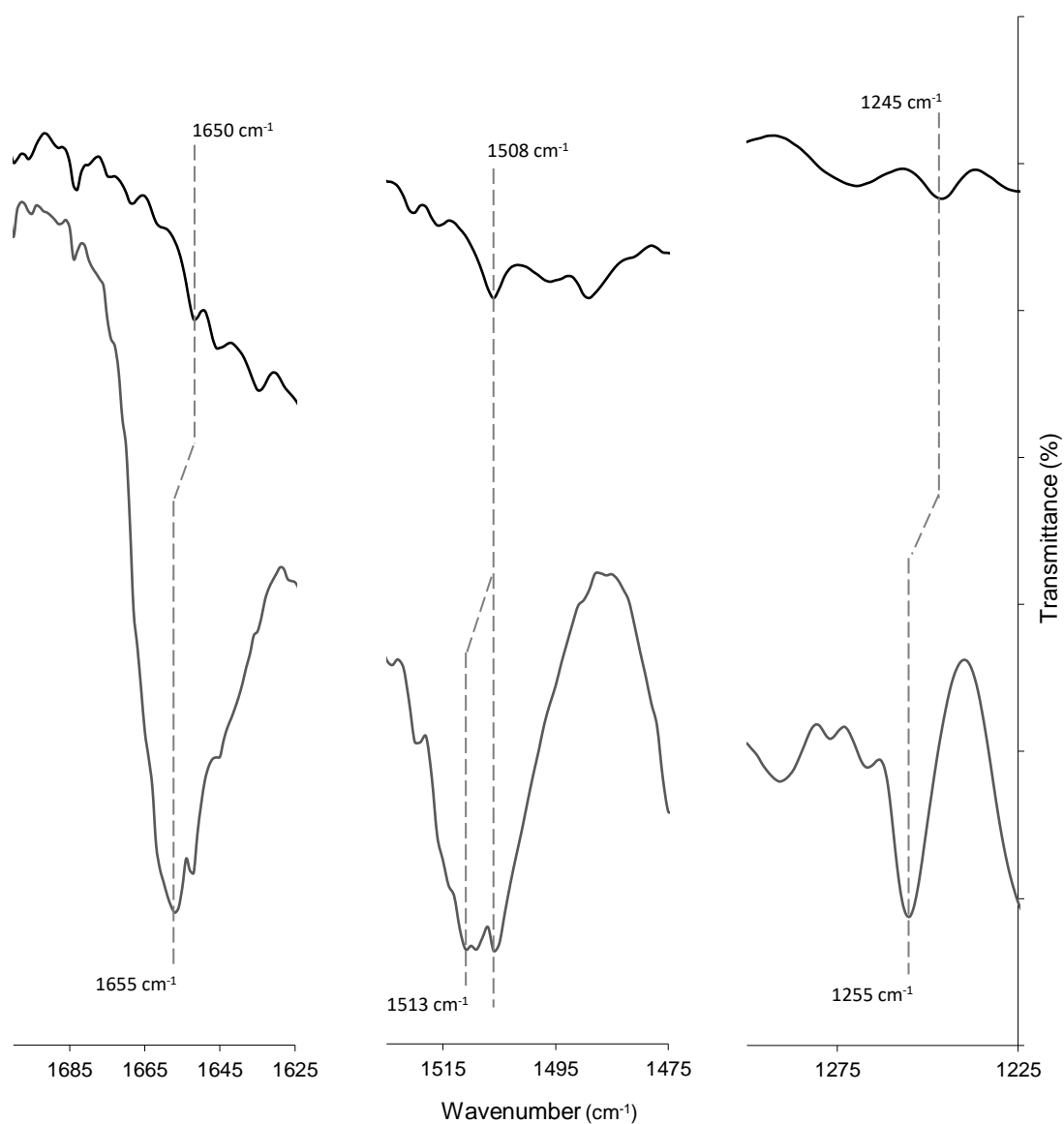


**Figure 5.** FTIR spectra for TC at pH 5 (grey line) and rMt-TC composite formed at pH 5 (black line). Absorbances are paired via the dashed lines indicating shifts.

The absorbance at  $1508\text{ cm}^{-1}$  is assigned to the amide II band, with a secondary peak at  $1513\text{ cm}^{-1}$  generally assigned to N-H stretch at the amide II group (Caminati et al., 2002; Chang et al., 2009a; Li et al., 2010; Parolo et al., 2008; Y. Zhao et al., 2012). The  $1508\text{ cm}^{-1}$  absorbance did not change position whilst the  $1513\text{ cm}^{-1}$  absorbance did not appear in the spectra for the composites, which could suggest there is no interaction between the clay-mineral and the amide groups. The amide group and O3 complex holds a negative charge above  $pK_{a1}$  (Parolo et al., 2008) and the shifting or disappearance of the  $1513\text{ cm}^{-1}$  absorbance, resulting in a single absorbance at  $1508\text{ cm}^{-1}$  could

indicate some interaction with this group and the positively charged edges of the clay mineral, providing the pH does not favour a negative charge at these edge sites. Further evidence for an interaction with the amide groups is presented in figure 5, which shows the amide C=O absorbance at  $1655\text{ cm}^{-1}$  (Li et al., 2010; Y. Zhao et al., 2012) shifting to  $1650\text{ cm}^{-1}$ .

### 3.5. X-ray diffraction analyses

The diffractograms for TC and DC represent a typical XRD pattern for crystalline materials. The diffractions in these two patterns are much more clearly defined and symmetric in comparison to the clay mineral diffractograms (figure 6). The low-intensity clay mineral diffraction peaks can be explained by their random orientation on the sample plate, rather than being artificially oriented (Villar et al., 2012; Zhou et al., 2018). No shift in the  $001$  reflection peak was observed for any of the clay minerals after they had been dispersed in water and dried in the same way as the composite materials. Physical mixes of the clay mineral and antibiotic powders provided diffractograms containing peaks for both the clay minerals and the antibiotic powders alone but showed no shift in diffraction and the  $001$  reflection remained intact. There was a notable lack of TC or DC diffraction peaks in the composite samples indicating the TC and DC molecules were adsorbed onto the clay mineral surfaces in an amorphous arrangement (Ito et al., 2001) and that the surfaces of the clay minerals did not act as foci for crystallisation of the antibiotics.

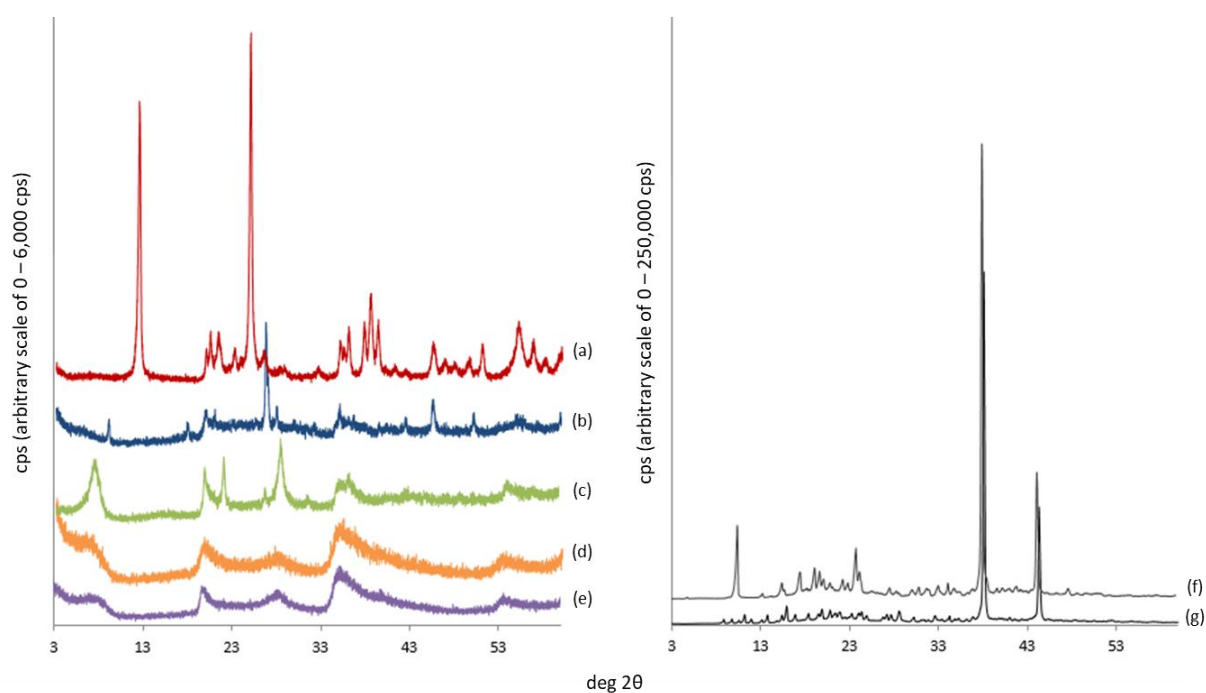


**Figure 6.** Stacked X-ray diffractograms of unmodified Kaol (a), MtK10 (b), rMT (c), LapRD (d), LapXL21 (e), DC (f), and TC (g). Relative scales are given next to each diffractogram.

The layers of Kaol are held tightly and closely together by hydrogen bonds, which makes them hard to separate (Miranda-Trevino and Coles, 2003). The adsorption of TC and DC onto Kaol resulted in no significant change in the shape or position of the *001* reflection (figure 7) indicating that neither of these antibiotics adsorbed into the interlayer space, which remained at 7.15 Å. TC and DC were more likely adsorbed onto the outer surfaces of the Kaol particles (Hamilton et al., 2014; Miranda-Trevino and Coles, 2003).

The *001* reflection in MtK10 also remained at the same position as the amount of antibiotic adsorbed increased, suggesting the structural changes brought about by acid activation inhibit the infiltration of TC and DC into any remaining interlayer space. However, this poorly defined basal reflection becomes less defined and absent as the antibiotic-load within the MtK10 composites increased. One explanation for this is adsorption onto the outer surface prevented the formation of normal clay mineral aggregates and thus the normal pseudo-crystalline structure (Janeba et al., 1998).

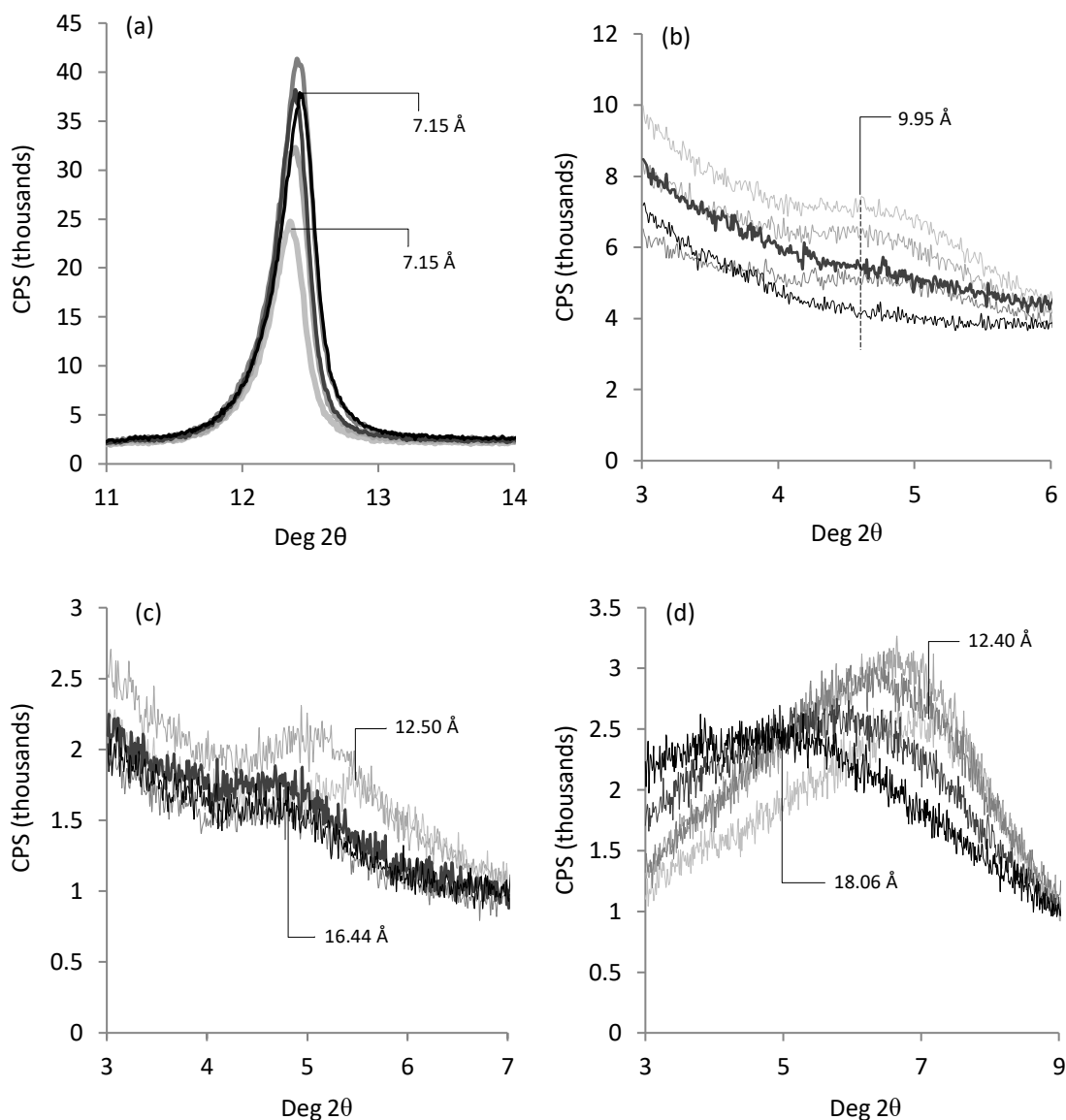


**Figure 7.** X-ray diffractions for DC adsorbed onto (a) Kaol, (b) MtK-10, (c) rMt, and (d) LapRD. Shading of the diffractograms represent different concentrations of DC loading, whereby black is the greatest antibiotic-loading and the lightest grey represents least antibiotic loading.

Figure 7 demonstrates changes in the shape and position of the *001* reflection as TC and DC were adsorbed in increasing amounts onto rMt and LapRD (data not shown for LapXL21 as very similar to LapRD). For these clay minerals the adsorption of TC and DC caused the *001* reflection to shift to the left, representing an increase in the size of the interlayer space (Chang et al., 2009b; Parolo et al., 2008). The increase in interlayer space was limited in rMt as the distance increased to, then remained at, 16.44 Å. As the antibiotic loading onto LapRD and LapXL21 increased further so did the interlayer space. For example, as TC loading onto LapRD increased from 8.31 mg/g to 83.14 mg/g then to 154.47 mg/g the interlayer space was found to be 12.70 Å, 13.97 Å, and 18.06 Å respectively.

The width and asymmetry of the LapRD and LapXL21 basal reflection also increased, suggesting that antibiotic molecules present within the interlayer space were able to exfoliate the mineral structure (Chang et al., 2009b).

### *3.6. Antibacterial activity*

Clay minerals on their own exhibited no zone of inhibition and therefore no discernible antibacterial activity (figure 8a). This is in contrast to other studies that showed varying inhibitory effects of some clay minerals on the growth of bacterial cells (Otto and Haydel, 2013; Williams et al., 2011). However, it is likely that close contact with bacterial cells is required for clay minerals to impose their antibacterial effects (Williams and Haydel, 2010), unlike in the experiments in our where the bacterial cells were largely separated from the clay minerals. The interlayer cations of the clay minerals tested were predominantly Na<sup>+</sup>, which has no inherent antibacterial activity unlike other metallic cations such as silver, copper and zinc (Gaskell and Hamilton, 2014).

As the concentration of TC and DC increased within each clay-antibiotic composite, the zone of inhibition also increased in diameter (figure 8b-d). These data prove that the antibacterial effects of TC and DC is maintained during the formation and storage of the clay-antibiotic composites and the assay performed was sensitive to the concentration of antibiotic released. As the concentration of the standard solutions of TC and DC increased so did the zone of inhibition, proving that this method could discriminate between clay-antibiotic composites that released TC and DC on rehydration and those that did not. By plotting the zone of inhibition (mm) against the Log<sub>10</sub> of TC and DC concentration (mg/mL) standard curves with high correlation ( $r^2 > 0.955$ ) were obtained, showing that this methodology could reliably detect increasing amounts of TC and DC release through increasing zone diameters.

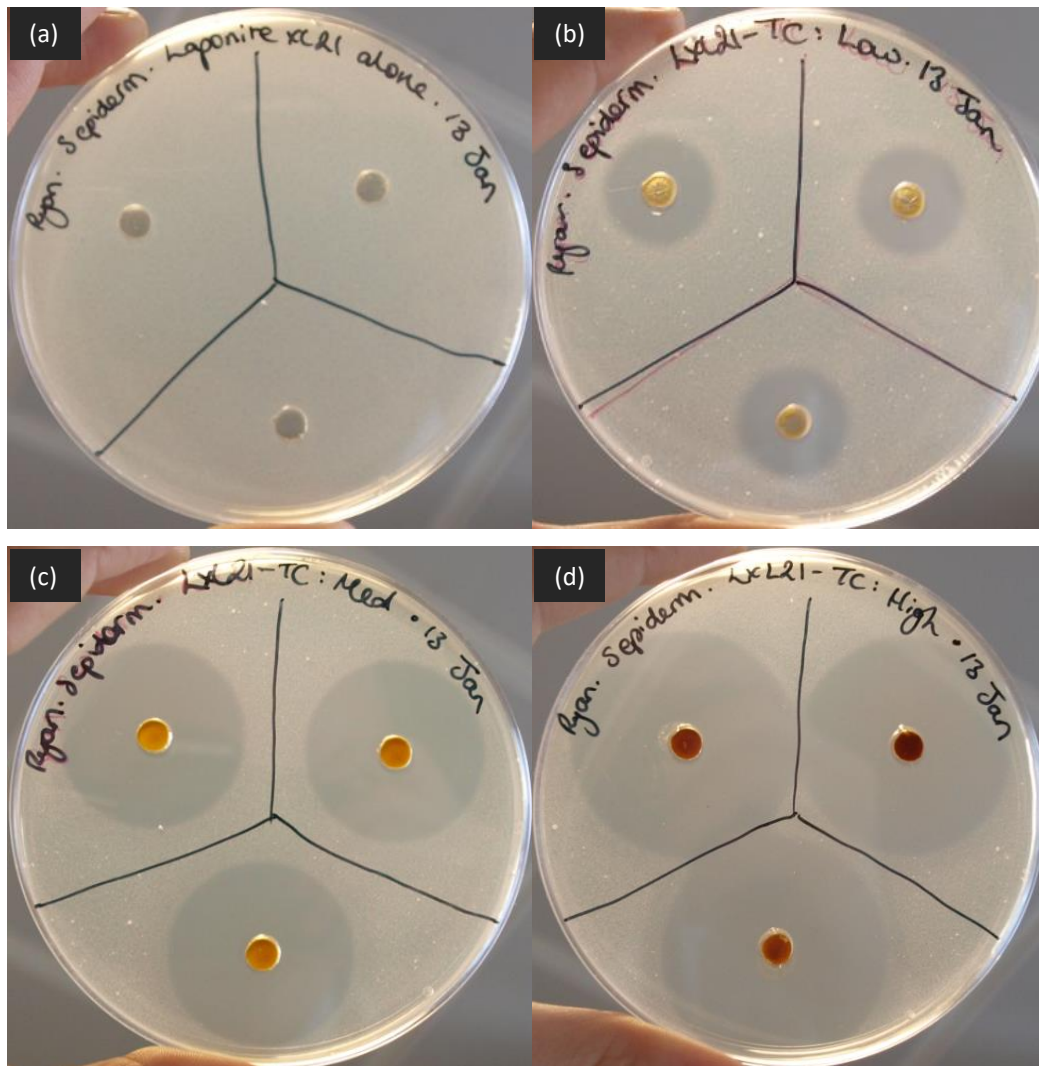


**Figure 8.** Examples of *S. epidermidis* cultures in nutrient agar tested via the well-diffusion method against 2 mg LapXL21 (A), and composites of LapXL21-TC containing 10.21 mg/g (B), 79.19 mg/g (C), and 124.15 mg/g of TC (D).

The diameters for the zones of inhibition were converted into areas of effect to give an expression of efficacy as the average number of cells effected (table 3). TC and DC were shown to have antibacterial effects against all the bacterial strains but were more effective against the Gram-positive strains due to their mode of action (Chatterjee et al., 2016; Kobayashi et al., 2009; Lister et al., 2009; Potron et al., 2015). It is important to note the reduced efficacy of TC and DC against *P. aeruginosa* compared to *C. acnes* and *S. epidermidis*. *Pseudomonas* spp. are Gram-negative bacteria which have less permeable cell membranes, which can reduce the penetration of many antibacterial agents. *P. aeruginosa* is able to produce a number of efflux proteins which are placed within the cell membranes to pump out a wide range of antibiotics including the tetracycline class. In addition to

this innate resistance *P. aeruginosa* is able to acquire and develop further resistance even during a course of anti-pseudomonal treatment (Chatterjee et al., 2016; Kobayashi et al., 2009; Lister et al., 2009; Potron et al., 2015).

**Table 3.** Calculated mean average number of bacterial cells that were prevented from growing by antibiotic molecules which had diffused from clay-TC and clay-DC composites of different antibiotic load.

Composite	Antibiotic Load (mg/g)	Average number of bacterial cells inhibited ( $\times 10^5$ )		
		<i>S. epidermidis</i>	<i>C. acnes</i>	<i>P. aeruginosa</i>
Kaol-TC	4.75	1.88	2.01	-
	14.97	2.75	4.00	2.53
	29.92	3.29	4.51	3.82
MtK10-TC	10.30	0.58	1.00	-
	98.19	2.90	3.95	-
	148.69	3.71	5.13	4.77
rMt-TC	10.01	0.24	1.25	-
	111.15	1.42	3.24	1.45
	158.06	1.86	4.71	5.99
LapRD-TC	9.82	0.59	0.21	-
	129.71	2.07	2.99	-
	199.75	2.61	3.65	-
LapXL21-TC	10.21	0.48	1.86	-
	79.19	1.58	4.47	0.54
	124.15	2.38	5.80	7.24
Kaol-DC	3.71	0.65	2.55	-
	9.83	1.40	5.06	-
	16.23	1.75	5.58	-
MtK10-DC	9.97	0.59	3.02	-
	114.81	2.07	5.18	3.64
	146.77	2.55	5.90	15.65
rMt-DC	9.71	0.54	1.98	-
	92.88	1.59	3.96	-
	133.70	2.10	4.97	5.05
LapRD-DC	7.00	0.31	1.67	-
	112.72	1.54	4.56	0.37
	175.36	1.90	5.55	4.81
LapXL21-DC	5.92	0.78	3.27	-
	82.96	1.58	4.78	-
	132.33	2.04	5.46	2.79

The calculated efficacy of preventing bacterial-cell growth increased by a smaller proportion when the antibiotic-load increased from medium to high than it did when the antibiotic-load increased from low to medium (table 3). This complements the trends observed in the zone of inhibition measurements, suggesting that diffusion through increasing volumes of agar was not solely responsible for this phenomenon. This assumption is further supported when the chemistry of each clay mineral is considered. Composites formed from Kaol were shown to create zones of inhibition

that were comparable to those formed by other composites, which is interesting given Kaol-TC and Kaol-DC composites contained much less antibiotic than many of the other composites tested. This suggests the interaction of Kaol (a 1:1 clay mineral) and these antibiotics is weaker than the highly charged 2:1 clay minerals (rMt and Laponites®). The composites with low TC and DC binding had not formed a monolayer and therefore the antibiotic molecules were interacting directly with the surface of the clay minerals through strong interactions. As the antibiotic loading increased to 'medium' and 'high' a monolayer had likely formed and additional antibiotic molecules would have adsorbed through secondary weaker interactions. However, these secondary interactions did not result in the antibiotic molecules being able to dissociate more easily away from the clay mineral surface.

One limitation of the method used to test the antibacterial activities of these composites is they are time-limited in a number of ways, which could have affected the zones of inhibition obtained. Firstly, the antibiotic needs to dissociate from the composite and diffuse through the surrounding agar, whilst bacterial cells proliferate. The zone of inhibition is formed at a boundary where the antibacterial concentration in the agar is strong enough to prevent bacterial growth, and those areas where it is not. Such bacteriostatic and bactericidal concentrations take time to develop, during which time the bacterial cells outside of the effective concentration continue to grow and replicate. Any bacterial colonies that are able to replicate to sufficient densities to be visible before TC and DC reach effective concentrations will still be visible after cell-death. Therefore, antibiotic may continue to diffuse through the agar but the true extent of antibiotic release cannot be measured.

Secondly, the TC and DC molecules can only desorb from the composite when it is hydrated. These bacteriological studies were carried out at body temperature, which facilitated gradual evaporation of water from the composite dispersions to such an extent that these were dry at 24-hours incubation time. This could also mask the true extent of antibiotic release from these composite materials especially if modified release properties are present, as has been reported by a number of other teams (Park et al., 2008; Rodrigues et al., 2013).

Regardless of these limitations the results are important as they show the clay-antibiotic composites formed are able to relinquish their TC and DC load and have a significant antibacterial effect, especially as the antibiotic-load increases.

#### **4. Conclusions**

TC and DC were successfully adsorbed onto Kaol, MtK10, rMt, LapRD and LapXL21 under various conditions. The adsorption of TC and DC was rapid and followed pseudo-second order kinetics. Adsorption isotherms suggested that these antibiotic molecules formed a monolayer on the clay mineral surfaces and further adsorption can occur via weaker secondary interactions. A dispersion pH that favoured the zwitterionic forms of TC and DC was shown to allow the greatest amount of adsorption onto the clay minerals. A dispersion pH that favoured negatively charged antibiotic molecules resulted in almost negligible TC or DC adsorption – likely a result of clay mineral edge-sites becoming negatively charged creating an overwhelming repulsion between the clay mineral layers and the antibiotic molecules.

Through XRD and FTIR it was determined that TC and DC adsorbed into the interlayer space of swelling 2:1 clay minerals but probably only adsorbed onto the outer surfaces of Kaol and MtK10. It is likely that the positively charged dimethyl amino group on these antibiotic molecules enabled direct interaction with the negatively charged clay-mineral surfaces. It is also possible that negatively charged amide groups could adsorb onto the positively charged edge-sites of the clay mineral layers. The clay-antibiotic composites showed antibacterial activity against *S. epidermidis*, *C. acnes* and *P. aeruginosa*. Increasing antibiotic-load within the composites resulted in greater antibacterial effect. Kaol, which has weak surface forces, was shown to relinquish its antibiotic load much more easily than the highly charged clay minerals.

Overall, the findings of these studies demonstrate these clay-antibiotic composites are suitable antibiotic-delivery materials with the ability to effectively release TC and DC and have a significant antibacterial effect proportional to the amount of antibiotic loaded. Future research will need to focus on elucidating TC and DC release profiles from these composite materials, determining cytocompatibility in relevant human cell-lines and overall toxicity in animal models, then developing and evaluating acceptable pharmaceutical formulations for use in skin and skin-structure infections.

## 5. References

- Aguzzi, C., Viseras, C., Cerezo, P., Rossi, S., Ferrari, F., López-Galindo, A., Caramella, C., 2005. Influence of dispersion conditions of two pharmaceutical grade clays on their interaction with some tetracyclines. *Appl. Clay Sci.* 30, 79–86. <https://doi.org/10.1016/j.clay.2005.03.007>
- Aguzzi, C., Viseras, C., Cerezo, P., Salcedo, I., Sánchez-Espejo, R., Valenzuela, C., 2013. Release kinetics of 5-aminosalicylic acid from halloysite. *Colloids Surf. B. Biointerfaces* 105, 75–80. <https://doi.org/10.1016/j.colsurfb.2012.12.041>
- Browne, J.E., Feldkamp, J.R., White, J.L., Hem, S.L., 1980. Acid-base equilibria of tetracycline in

sodium montmorillonite suspensions. *J. Pharm. Sci.* 69, 811–5.

- Caminati, G., Focardi, C., Gabrielli, G., Gambinossi, F., Mecheri, B., Nocentini, M., Puggelli, M., 2002. Spectroscopic investigation of tetracycline interaction with phospholipid Langmuir–Blodgett films. *Mater. Sci. Eng. C* 22, 301–305. [https://doi.org/10.1016/S0928-4931\(02\)00217-5](https://doi.org/10.1016/S0928-4931(02)00217-5)
- Chang, P.-H., Jean, J.-S., Jiang, W.-T., Li, Z., 2009a. Mechanism of tetracycline sorption on rectorite. *Colloids Surfaces A Physicochem. Eng. Asp.* 339, 94–99. <https://doi.org/10.1016/j.colsurfa.2009.02.002>
- Chang, P.-H., Li, Z., Jiang, W.-T., Jean, J.-S., 2009b. Adsorption and intercalation of tetracycline by swelling clay minerals. *Appl. Clay Sci.* 46, 27–36. <https://doi.org/10.1016/j.clay.2009.07.002>
- Chang, P.-H., Li, Z., Yu, T.-L., Munkhbayer, S., Kuo, T.-H., Hung, Y.-C., Jean, J.-S., Lin, K.-H., 2009c. Sorptive removal of tetracycline from water by palygorskite. *J. Hazard. Mater.* 165, 148–55. <https://doi.org/10.1016/j.jhazmat.2008.09.113>
- Chatterjee, M., Anju, C.P., Biswas, L., Anil Kumar, V., Gopi Mohan, C., Biswas, R., 2016. Antibiotic resistance in *Pseudomonas aeruginosa* and alternative therapeutic options. *Int. J. Med. Microbiol.* 306, 48–58. <https://doi.org/10.1016/j.ijmm.2015.11.004>
- Chen, Y., Zhou, A., Liu, B., Liang, J., 2010. Tramadol hydrochloride/montmorillonite composite: Preparation and controlled drug release. *Appl. Clay Sci.* 49, 108–112. <https://doi.org/10.1016/j.clay.2010.04.011>
- Davies, S.C., 2013. Annual Report of the Chief Medical Officer, Volume Two, 2011, Infections and the rise of antimicrobial resistance. Department of Health, London.
- Dawson, A.L., Dellavalle, R.P., 2013. Acne vulgaris. *BMJ* 346, f2634. <https://doi.org/10.1136/bmj.f2634>
- de Sousa, F.B., Oliveira, M.F., Lula, I.S., Sansiviero, M.T.C., Cortés, M.E., Sinisterra, R.D., 2008. Study of inclusion compound in solution involving tetracycline and  $\beta$ -cyclodextrin by FTIR-ATR. *Vib. Spectrosc.* 46, 57–62. <https://doi.org/10.1016/j.vibspec.2007.10.002>
- Deng, Y., Velázquez, A.L.B., Billes, F., Dixon, J.B., 2010. Bonding mechanisms between aflatoxin B1 and smectite. *Appl. Clay Sci.* 50, 92–98. <https://doi.org/10.1016/j.clay.2010.07.008>
- Figueroa, R. a, Leonard, A., MacKay, A. a, 2004. Modeling tetracycline antibiotic sorption to clays. *Environ. Sci. Technol.* 38, 476–83.
- Gaskell, E.E., Hamilton, A.R., 2014. Antimicrobial clay-based materials for wound care. *Future Med. Chem.* 6, 641.
- Ghezzi, L., Spepi, A., Agnolucci, M., Cristani, C., Giovannetti, M., Tiné, M.R., Duce, C., 2018. Kinetics of release and antibacterial activity of salicylic acid loaded into halloysite nanotubes. *Appl. Clay Sci.* 160, 88–94. <https://doi.org/10.1016/j.clay.2017.11.041>
- Grassi, G.G., 1993. Tetracyclines — extending the atypical spectrum. *Int. J. Antimicrob. Agents* 3, S31–S46. [https://doi.org/10.1016/0924-8579\(93\)90033-2](https://doi.org/10.1016/0924-8579(93)90033-2)
- Greenwald, R. a, 2011. The road forward: the scientific basis for tetracycline treatment of arthritic disorders. *Pharmacol. Res.* 64, 610–3. <https://doi.org/10.1016/j.phrs.2011.06.010>
- Griffin, M.O., Fricovsky, E., Ceballos, G., Villarreal, F., 2010. Tetracyclines : a pleiotropic family of compounds with promising therapeutic properties . Review of the literature. *AM J Physiol Cell*

- Physiol 299, C539–C548. <https://doi.org/10.1152/ajpcell.00047.2010>.
- Hamilton, A.R., Hutcheon, G.A., Roberts, M., Gaskell, E.E., 2014. Formulation and antibacterial profiles of clay – ciprofloxacin composites. *Appl. Clay Sci.* 87, 129–135. <https://doi.org/10.1016/j.clay.2013.10.020>
- Ito, T., Sugafuji, T., Maruyama, M., 2001. Skin Penetration by Indomethacin is Enhanced by Use of an Indomethacin / Smectite Complex. *J. Supramol. Chem.* 1 217–219.
- Itodo, A.U., Itodo, H.U., 2010. Sorption energies estimation using Dubinin-Radushkevich and temkin adsorption isotherms. *Life Sci. J.* 7, 68–76.
- Janeba, D., Capkova, P., Weiss, Z., Schenk, H., 1998. Characterization of intercalated smectites using xrd profile analysis in the low-angle region. *Clays Clay Miner.* 46, 63–68.
- Joks, R., Durkin, H.G., 2011. Non-antibiotic properties of tetracyclines as anti-allergy and asthma drugs. *Pharmacol. Res.* 64, 602–9. <https://doi.org/10.1016/j.phrs.2011.04.001>
- Kammerer, J., Carle, R., Kammerer, D.R., 2011. Adsorption and Ion Exchange: Basic Principles and Their Application in Food Processing. *J. Agric. Food Chem.* 59, 22–42. <https://doi.org/10.1021/jf1032203>
- Kobayashi, H., Kobayashi, O., Kawai, S., 2009. Pathogenesis and clinical manifestations of chronic colonization by *Pseudomonas aeruginosa* and its biofilms in the airway tract. *J. Infect. Chemother.* 15, 125–142. <https://doi.org/10.1007/s10156-008-0691-3>
- Lagaly, G., Ziesmer, S., 2003. Colloid chemistry of clay minerals: the coagulation of montmorillonite dispersions. *Adv. Colloid Interface Sci.* 100–102, 105–128. [https://doi.org/10.1016/S0001-8686\(02\)00064-7](https://doi.org/10.1016/S0001-8686(02)00064-7)
- Li, Z., Chang, P.-H., Jean, J.-S., Jiang, W.-T., Wang, C.-J., 2010. Interaction between tetracycline and smectite in aqueous solution. *J. Colloid Interface Sci.* 341, 311–9. <https://doi.org/10.1016/j.jcis.2009.09.054>
- Lipson, S.M., Stotzky, G., 1983. Adsorption of Reovirus to Clay Minerals: Effects of Cation-Exchange Capacity, Cation Saturation, and Surface Area. *Appl. Environ. Microbiol.* 46, 673–682.
- Lister, P.D., Wolter, D.J., Hanson, N.D., 2009. Antibacterial-resistant *Pseudomonas aeruginosa*: Clinical impact and complex regulation of chromosomally encoded resistance mechanisms. *Clin. Microbiol. Rev.* 22, 582–610. <https://doi.org/10.1128/CMR.00040-09>
- Madejova, J., 2003. FTIR techniques in clay mineral studies. *Vib. Spectrosc.* 31, 1–10.
- Miranda-Trevino, J.C., Coles, C.A., 2003. Kaolinite properties, structure and influence of metal retention on pH. *Appl. Clay Sci.* 23, 133–139. [https://doi.org/10.1016/S0169-1317\(03\)00095-4](https://doi.org/10.1016/S0169-1317(03)00095-4)
- Monk, E., Shalita, A., Siegel, D.M., 2011. Clinical applications of non-antimicrobial tetracyclines in dermatology. *Pharmacol. Res.* 63, 130–45. <https://doi.org/10.1016/j.phrs.2010.10.007>
- Neumann, B.S., Sansom, K.G., 1971. The rheological properties of dispersions of Laponite, a synthetic hectorite-like clay, in electrolyte solutions. *Clay Miner.* 9, 231–243.
- Otto, C.C., Haydel, S.E., 2013. Exchangeable ions are responsible for the in vitro antibacterial properties of natural clay mixtures. *PLoS One* 8, e64068. <https://doi.org/10.1371/journal.pone.0064068>

- Pan, Q., Li, N., Hong, Y., Tang, H., Zheng, Z., Weng, S., Zheng, Y., Huang, L., 2017. Halloysite clay nanotubes as effective nanocarriers for the adsorption and loading of vancomycin for sustained release. *RSC Adv.* 7. <https://doi.org/10.1039/c7ra00376e>
- Park, J.K., Choy, Y. Bin, Oh, J.-M., Kim, J.Y., Hwang, S.-J., Choy, J.-H., 2008. Controlled release of donepezil intercalated in smectite clays. *Int. J. Pharm.* 359, 198–204. <https://doi.org/10.1016/j.ijpharm.2008.04.012>
- Parolo, M.E., Avena, M.J., Pettinari, G., Zajonkovsky, I., Valles, J.M., Baschini, M.T., 2010. Antimicrobial properties of tetracycline and minocycline-montmorillonites. *Appl. Clay Sci.* 49, 194–199. <https://doi.org/10.1016/j.clay.2010.05.005>
- Parolo, M.E., Avena, M.J., Savini, M.C., Baschini, M.T., Nicotra, V., 2013. Adsorption and circular dichroism of tetracycline on sodium and calcium-montmorillonites. *Colloids Surfaces A Physicochem. Eng. Asp.* 417, 57–64. <https://doi.org/10.1016/j.colsurfa.2012.10.060>
- Parolo, M.E., Savini, M.C., Vallés, J.M., Baschini, M.T., Avena, M.J., 2008. Tetracycline adsorption on montmorillonite: pH and ionic strength effects. *Appl. Clay Sci.* 40, 179–186. <https://doi.org/10.1016/j.clay.2007.08.003>
- Porubcan, L.S., Serna, C.J., White, J.L., Hem, S.L., 1978. Mechanism of Adsorption of Clindamycin and Tetracycline by Montmorillonite. *J. Pharm. Sci.* 67, 1081–1087.
- Potron, A., Poirel, L., Nordmann, P., 2015. Emerging broad-spectrum resistance in *Pseudomonas aeruginosa* and *Acinetobacter baumannii*: Mechanisms and epidemiology. *Int. J. Antimicrob. Agents* 45, 568–585. <https://doi.org/10.1016/j.ijantimicag.2015.03.001>
- Puttamat, S., Pavarajarn, V., 2016. Adsorption study for removal of Mn(II) ion in aqueous solution by hydrated ferric(III) oxides. *Int. J. Chem. Eng. Appl.* 7, 239–243. <https://doi.org/10.18178/ijcea.2016.7.4.581>
- Qiang, Z., Adams, C., 2004. Potentiometric determination of acid dissociation constants (pKa) for human and veterinary antibiotics. *Water Res.* 38, 2874–90. <https://doi.org/10.1016/j.watres.2004.03.017>
- Rapacz-kmita, A., Bu, M.M., Stodolak-zych, E., Miko, M., Dudek, P., Trybus, M., 2017. Characterisation, in vitro release study, and antibacterial activity of montmorillonite-gentamicin complex material. *Mater. Sci. Eng. C* 70, 471–478. <https://doi.org/10.1016/j.msec.2016.09.031>
- Raza, M., Ballering, J.G., Hayden, J.M., Robbins, R. a, Hoyt, J.C., 2006. Doxycycline decreases monocyte chemoattractant protein-1 in human lung epithelial cells. *Exp. Lung Res.* 32, 15–26. <https://doi.org/10.1080/01902140600691399>
- Rivera, A., Valdés, L., Jiménez, J., Pérez, I., Lam, A., Altshuler, E., De Ménorval, L.C., Fossum, J.O., Hansen, E.L., Rozynek, Z., 2016. Smectite as ciprofloxacin delivery system: Intercalation and temperature-controlled release properties. *Appl. Clay Sci.* 124–125, 150–156. <https://doi.org/10.1016/j.clay.2016.02.006>
- Rodrigues, L.A.D.S., Figueiras, A., Veiga, F., de Freitas, R.M., Nunes, L.C.C., da Silva Filho, E.C., da Silva Leite, C.M., 2013. The systems containing clays and clay minerals from modified drug release: a review. *Colloids Surf. B. Biointerfaces* 103, 642–51. <https://doi.org/10.1016/j.colsurfb.2012.10.068>
- Rong, X., Huang, Q., He, X., Chen, H., Cai, P., Liang, W., 2008. Interaction of *Pseudomonas putida*

- with kaolinite and montmorillonite: a combination study by equilibrium adsorption, ITC, SEM and FTIR. *Colloids Surf. B. Biointerfaces* 64, 49–55.  
<https://doi.org/10.1016/j.colsurfb.2008.01.008>
- Samlíková, M., Hole, S., Hundáková, M., Pazdziora, E., Valá, M., 2017. Preparation of antibacterial chlorhexidine / vermiculite and release study. *Int. J. Miner. Process.* 159, 1–6.  
<https://doi.org/10.1016/j.minpro.2016.12.002>
- Sandwell and West Birmingham Hospitals NHS Trust, 2011. Antimicrobial Prescribing Formulary. Birmingham City Hospital, Birmingham (UK), [Internal Document].
- Schiffenbauer, M., Stotzky, G., 1982. Adsorption of coliphages T1 and T7 to Clay Minerals. *Appl. Environ. Microbiol.* 43, 590–596.
- Segad, M., Jönsson, B., Akesson, T., Cabane, B., 2010. Ca/Na montmorillonite: structure, forces and swelling properties. *Langmuir* 26, 5782–90. <https://doi.org/10.1021/la9036293>
- Swartzen-Allen, S.L., Matijevic, E., 1974. Surface and colloid chemistry of clays. *Chem. Rev.* 74, 385–400. <https://doi.org/10.1021/cr60289a004>
- Tan, D., Yuan, P., Annabi-bergaya, F., Liu, D., Wang, L., Liu, H., He, H., 2014. Loading and in vitro release of ibuprofen in tubular halloysite. *Appl. Clay Sci.* 96, 50–55.  
<https://doi.org/10.1016/j.clay.2014.01.018>
- The Royal Liverpool and Broadgreen University Hospitals NHS Trust, 2012. Skin and Soft Tissue Infections Prescribing Guidance. Royal Liverpool University Hospital, Liverpool (UK), [Internal Document].
- Thompson, D.W., Butterworth, J.T., 1992. The Nature of Laponite and Its Aqueous Dispersions. *J. Colloid Interface Sci.* 151, 236–243.
- Tsankov, N., Broshtilova, V., Kazandjieva, J., 2003. Tetracyclines in dermatology. *Clin. Dermatol.* 21, 33–39. [https://doi.org/10.1016/S0738-081X\(02\)00324-3](https://doi.org/10.1016/S0738-081X(02)00324-3)
- Tyagi, B., Chudasama, C.D., Jasra, R. V, 2006. Determination of structural modification in acid activated montmorillonite clay by FT-IR spectroscopy. *Spectrochim. Acta. A. Mol. Biomol. Spectrosc.* 64, 273–8. <https://doi.org/10.1016/j.saa.2005.07.018>
- Villar, M.V., Gómez-Espina, R., Gutiérrez-Nebot, L., 2012. Basal spacings of smectite in compacted bentonite. *Appl. Clay Sci.* 65–66, 95–105. <https://doi.org/10.1016/j.clay.2012.05.010>
- Viseras, C., Aguzzi, C., Cerezo, P., Lopezgalindo, A., 2007. Uses of clay minerals in semisolid health care and therapeutic products. *Appl. Clay Sci.* 36, 37–50.  
<https://doi.org/10.1016/j.clay.2006.07.006>
- Viseras, C., Cerezo, P., Sanchez, R., Salcedo, I., Aguzzi, C., 2010. Current challenges in clay minerals for drug delivery. *Appl. Clay Sci.* 48, 291–295. <https://doi.org/10.1016/j.clay.2010.01.007>
- Wang, Q., Zhang, J., Zheng, Y., Wang, A., 2014. Adsorption and release of ofloxacin from acid- and heat-treated halloysite. *Colloids Surf. B. Biointerfaces* 113, 51–8.  
<https://doi.org/10.1016/j.colsurfb.2013.08.036>
- Williams, L.B., Haydel, S.E., 2010. Evaluation of the medicinal use of clay minerals as antibacterial agents. *Int. Geol. Rev.* 52, 745–770. <https://doi.org/10.1080/00206811003679737>
- Williams, L.B., Metge, D.W., Eberl, D.D., Harvey, R.W., Turner, A.G., Prapaipong, P., Poret-Peterson,

A.T., 2011. What makes a natural clay antibacterial? *Environ. Sci. Technol.* 45, 3768–73.  
<https://doi.org/10.1021/es1040688>

World Health Organization, 2012. The evolving threat of antimicrobial resistance: Options for action. World Health Organization, Switzerland.

Yuan, P., Tan, D., Annabi-Bergaya, F., 2015. Properties and applications of halloysite nanotubes: recent research advances and future prospects. *Appl. Clay Sci.* 112–113, 75–93.  
<https://doi.org/10.1016/j.clay.2015.05.001>

Zhang, D., Zhou, C.-H., Lin, C.-X., Tong, D.-S., Yu, W.-H., 2010. Synthesis of clay minerals. *Appl. Clay Sci.* 50, 1–11. <https://doi.org/10.1016/j.clay.2010.06.019>

Zhao, W., Liu, X., Huang, Q., Walker, S.L., Cai, P., 2012. Interactions of pathogens *Escherichia coli* and *Streptococcus suis* with clay minerals. *Appl. Clay Sci.* 69, 37–42.  
<https://doi.org/10.1016/j.clay.2012.07.003>

Zhao, Y., Gu, X., Gao, S., Geng, J., Wang, X., 2012. Adsorption of tetracycline (TC) onto montmorillonite: Cations and humic acid effects. *Geoderma* 183–184, 12–18.  
<https://doi.org/10.1016/j.geoderma.2012.03.004>

Zhou, X., Liu, D., Bu, H., Deng, L., Liu, H., Yuan, P., Du, P., Song, H., 2018. XRD-based quantitative analysis of clay minerals using reference intensity ratios, mineral intensity factors, Rietveld, and full pattern summation methods: A critical review. *Solid Earth Sci.* 3, 16–29.  
<https://doi.org/10.1016/J.SESCI.2017.12.002>